

# Safety, Biodistribution, and Radiation Dosimetry of <sup>68</sup>Ga-OPS202 in Patients with Gastroenteropancreatic Neuroendocrine Tumors: A Prospective Phase I Imaging Study

Guillaume P. Nicolas<sup>1,2</sup>, Seval Beykan<sup>3</sup>, Hakim Bouterfa<sup>4</sup>, Jens Kaufmann<sup>4</sup>, Andreas Bauman<sup>5</sup>, Michael Lassmann<sup>3</sup>, Jean Claude Reubi<sup>6</sup>, Jean E.F. Rivier<sup>7</sup>, Helmut R. Maecke<sup>8</sup>, Melpomeni Fani<sup>1,5</sup>, and Damian Wild<sup>1,2</sup>

<sup>1</sup>Division of Nuclear Medicine, University Hospital Basel, Basel, Switzerland; <sup>2</sup>Center for Neuroendocrine and Endocrine Tumors, University Hospital Basel, Basel, Switzerland; <sup>3</sup>Department of Nuclear Medicine, University Hospital Würzburg, Würzburg, Germany; <sup>4</sup>OctreoPharm Sciences GmbH, Ipsen Group, Berlin, Germany; <sup>5</sup>Division of Radiopharmaceutical Chemistry, University Hospital Basel, Basel, Switzerland; <sup>6</sup>Cell Biology and Experimental Cancer Research, University of Berne, Berne, Switzerland; <sup>7</sup>Clayton Foundation Laboratories for Peptide Biology, Salk Institute, La Jolla, California; and <sup>8</sup>Department of Nuclear Medicine, University Hospital Freiburg, Freiburg, Germany

See an invited perspective on this article on page 907.

Preclinical and preliminary clinical evidence indicates that radiolabeled somatostatin (sst) receptor antagonists perform better than agonists in detecting neuroendocrine tumors (NETs). We performed a prospective phase I/II study to evaluate the sst receptor antagonist <sup>68</sup>Ga-OPS202 (<sup>68</sup>Ga-NODAGA-JR11; NODAGA = 1,4,7-triazacyclononane, 1-glutaric acid-4,7-acetic acid and JR11 = Cpa-c(DCys-Aph(Hor)-Daph(Cbm)-Lys-Thr-Cys-DTyr-NH<sub>2</sub>)) for PET imaging. Here, we report the results of phase I of the study. **Methods:** Patients received 2 single 150-MBq intravenous injections of <sup>68</sup>Ga-OPS202 3–4 wk apart (15 μg of peptide at visit 1 and 50 μg at visit 2). At visit 1, a dynamic PET/CT scan over the kidney was obtained during the first 30 min after injection, and static whole-body scans were obtained at 0.5, 1, 2, and 4 h after injection; at visit 2, a static whole-body scan was obtained at 1 h. Blood samples and urine were collected at regular intervals to determine <sup>68</sup>Ga-OPS202 pharmacokinetics. Safety, biodistribution, radiation dosimetry, and the most appropriate imaging time point for <sup>68</sup>Ga-OPS202 were assessed. **Results:** Twelve patients with well-differentiated gastroenteropancreatic (GEP) NETs took part in the study. <sup>68</sup>Ga-OPS202 cleared rapidly from the blood, with a mean residence time of 2.4 ± 1.1 min/L. The organs with the highest mean dose coefficients were the urinary bladder wall, kidneys, and spleen. The calculated effective dose was 2.4E–02 ± 0.2E–02 mSv/MBq, corresponding to 3.6 mSv, for a reference activity of 150 MBq. Based on total numbers of detected malignant lesions, the optimal time window for the scan was between 1 and 2 h. For malignant liver lesions, the time point at which most patients had the highest mean tumor contrast was 1 h. <sup>68</sup>Ga-OPS202 was well tolerated; adverse events were grade 1 or 2, and there were no signals of concern from laboratory blood or urinalysis tests. **Conclusion:** <sup>68</sup>Ga-OPS202 showed favorable biodistribution and imaging properties, with optimal tumor contrast between 1 and 2 h after injection. Dosimetry analysis revealed that the dose delivered by <sup>68</sup>Ga-OPS202

to organs is similar to that delivered by other <sup>68</sup>Ga-labeled sst analogs. Further evaluation of <sup>68</sup>Ga-OPS202 for PET/CT imaging of NETs is therefore warranted.

**Key Words:** neuroendocrine tumors; somatostatin receptor antagonist; dosimetry; <sup>68</sup>Ga-OPS202; <sup>68</sup>Ga-NODAGA-JR11

**J Nucl Med 2018; 59:909–914**

DOI: 10.2967/jnumed.117.199737

**N**euroendocrine tumors (NETs) can occur in almost any organ but are most common in the pancreas and gastrointestinal tract (1). Diagnosis is delayed by 3–10 y on average (2), and an estimated 40%–95% of gastroenteropancreatic NETs are metastatic by the time of diagnosis (3). Excluding benign insulinomas, more than 90% of all gastroenteropancreatic NETs express a high density of somatostatin receptor subtype 2 (sst<sub>2</sub> receptor) (4). As such, sst receptors have been exploited as molecular targets for imaging and treating gastroenteropancreatic NETs. Indeed, the use of radiolabeled sst analogs has become an integral part of the management of patients with these tumors, facilitating localization of the primary tumor, staging, and restaging (3). They can also be used as theranostic agents to determine the level of sst receptor expression and to select and treat appropriate patients with unlabeled or radiolabeled sst analogs (5).

sst receptor imaging was initially developed using scintigraphy or SPECT with <sup>111</sup>In- or <sup>99m</sup>Tc-labeled sst receptor agonists (6). Until recently, <sup>111</sup>In-pentetreotide (OctreoScan; Mallinckrodt, Inc.) was the most widely used radiolabeled sst analog. Currently, PET/CT using <sup>68</sup>Ga-DOTATOC is associated with a significantly higher detection rate than conventional sst receptor scintigraphy (6). This difference reflects the higher scanner sensitivity and spatial resolution of PET/CT than of SPECT (6), as well as the higher affinity of <sup>68</sup>Ga-DOTATOC for the sst<sub>2</sub> receptor (7). Alternatively, <sup>68</sup>Ga-DOTATATE has diagnostic accuracy comparable to <sup>68</sup>Ga-DOTATOC (8). In a direct comparison of <sup>68</sup>Ga-DOTATOC PET/CT and triple-phase CT, specificity was 97.4%, but sensitivity was only 72.8% in a lesion-based analysis (9). High diagnostic sensitivity is mandatory

Received Jul. 25, 2017; revision accepted Sep. 30, 2017.

For correspondence or reprints contact: Damian Wild, Division of Nuclear Medicine, University Hospital Basel, Petersgraben 4, CH-4031 Basel, Switzerland.

E-mail: damian.wild@usb.ch

Published online Oct. 12, 2017.

COPYRIGHT © 2018 by the Society of Nuclear Medicine and Molecular Imaging.

for planning surgery and other treatments; thus, there is a clinical need for further improvement of sst receptor imaging in patients with gastroenteropancreatic NETs.

The use of radiolabeled antagonists rather than agonists has the potential to improve sst receptor PET/CT imaging, because antagonists may recognize a higher number of sst receptor binding sites (10). Furthermore, in the first clinical study of the sst receptor antagonist <sup>111</sup>In-DOTA-BASS in cancer patients, tumor uptake and lesion detection rates were higher than with <sup>111</sup>In-pentetreotide (11). However, <sup>111</sup>In-DOTA-BASS is a SPECT tracer, with the above-described limitations of such tracers. For this reason, a small library of sst<sub>2</sub> receptor antagonists was developed for PET/CT imaging; of these, we selected OPS202 (NODAGA-JR11; NODAGA = 1,4,7-triazacyclononane,1-glutaric acid-4,7-acetic acid and JR11 = Cpa-c(DCys-Aph(Hor)-DAph(Cbm)-Lys-Thr-Cys)-DTyr-NH<sub>2</sub>) because it has demonstrated the highest affinity for sst<sub>2</sub> receptor when labeled with <sup>68</sup>Ga (12,13). The results of an in vivo biodistribution study comparing <sup>68</sup>Ga-DOTATATE (agonist) with <sup>68</sup>Ga-OPS202 and <sup>68</sup>Ga-DOTA-JR11 have shown that <sup>68</sup>Ga-OPS202 is the radiopharmaceutical of choice for clinical translation, on the basis of its very high tumor uptake and excellent biodistribution profile (13). Here, we present the results of the phase I component of a phase I/II study. Phase I evaluated the safety, biodistribution, radiation dosimetry, and optimal imaging time point of <sup>68</sup>Ga-OPS202 in patients with gastroenteropancreatic NETs.

## MATERIALS AND METHODS

### Study Design

This was an open-label microdosing phase I/II study performed at a single specialist center in Basel, Switzerland (ClinicalTrials.gov identifier NCT02162446; EudraCT no. 2014-001881-88). The Institutional Review Board approved the study, and all subjects signed a written informed consent form in accordance with the Declaration of Helsinki. There were 4 study visits: a screening visit; visit 1 (within 28 d of the screening visit), during which the first dose of <sup>68</sup>Ga-OPS202 (15 μg, 9.03 nmol of OPS202) was administered; visit 2 (3–4 wk after visit 1), during which the second dose of <sup>68</sup>Ga-OPS202 (50 μg, 30.1 nmol of OPS202) was administered; and the end-of-study visit 3 (7–15 d after visit 2) for follow-up.

### Patients

The main inclusion criteria were an age of at least 18 y, a histologically confirmed diagnosis of well-differentiated gastroenteropancreatic NET, a Karnofsky status of at least 60, a diagnostic CT/MRI scan of the tumor region and a positive sst receptor scan (<sup>68</sup>Ga-DOTATOC PET/CT) obtained in the previous 6 mo, no more than 30 lesions per organ, and at least 10% of the liver in a tumor-free state. Patients were excluded if they had previous or current allergic or autoimmune disease, active infection at screening or serious infection in the previous 6 mo, or treatment with NET-specific agents between the last sst receptor scan and the start of the study (excepting sst analogs, provided there was a sufficient washout period [28 d for long-acting somatostatin analogs and 2 d for short-acting somatostatin analogs]).

### Synthesis and Radiolabeling

OPS202 was synthesized according to good manufacturing practice by Bachem AG. <sup>68</sup>Ga-OPS202 was prepared on an automated synthesis unit (PharmTracer; Eckert and Ziegler) by loading the eluate of a <sup>68</sup>Ge/<sup>68</sup>Ga-generator (GalliaPharm; Eckert and Ziegler) onto a cation exchange column. <sup>68</sup>Ga was eluted with a mixture of 5 M NaCl/HCl (14) directly into a reaction vial containing an adjusted amount of OPS202, depending on the intended amount to be administered. OPS202 was radiolabeled at

75°C within 400 s, followed by C18 solid-phase extraction, with radiochemical purity of at least 95%.

### Imaging

The first administration of <sup>68</sup>Ga-OPS202 (visit 1) was 15 μg/150 MBq ± 25% intravenously over no longer than 1 min (the actual mean administered amount of peptide was 14 ± 4 μg [range, 11–19 μg], and the actual mean administered activity was 161 ± 21 MBq [range, 125–189 MBq]). The second administration of <sup>68</sup>Ga-OPS202 (visit 2) was 50 μg/150 MBq ± 25% (the actual mean administered amount of peptide was 50 ± 15 μg [range, 37–63 μg], and the actual mean administered activity was 172 ± 14 MBq [range, 141–192 MBq]). Except for diuretics, use of other medication on scan days was permitted. After injection, the cannula was flushed with normal saline and removed from the patient to measure the residual activity (including the syringe).

Three-dimensional PET scans were acquired at visits 1 and 2, using the same PET/CT scanner at both visits (Discovery STE; GE Healthcare). The effective administered activity (defined as the activity in the syringe before injection minus residual activity in the empty syringe after injection) was used for PET image reconstruction. Calibration and quality assurance were performed with <sup>68</sup>Ga in analogy to the EARL (European Association of Nuclear Medicine Research Ltd.) accreditation procedure with <sup>18</sup>F-FDG (<http://earl.eanm.org/cms/website.php>): the scanner was cross-calibrated to a well counter calibrated for <sup>68</sup>Ga using a homogeneously filled phantom; image quality and resolution were assessed using a National Electrical Manufacturers Association phantom with spheres of various size.

A low-dose, nonenhanced CT scan was acquired using 120 keV, current modulation (Smart mA [GE Healthcare], 30–300) of 0.8 s/rotation, and pitch of 1.75. All PET scans were acquired at 4 min/bed position with a 5-slice overlap. Attenuation-corrected PET images were reconstructed using the standard GE Healthcare proprietary 3-dimensional iterative reconstruction (3 mm in full width at half maximum, 21 subsets, 2 iterations, and 128 × 128 matrix, for a 70-cm-diameter field of view).

At visit 1, a dynamic scan was obtained over the kidney region during the first 30 min; static scans were obtained from head to sublingual

**TABLE 1**  
Baseline Demography and Disease Characteristics  
in the 12 Patients

Parameter	Data
Mean age (y)	54.8 (SD, 14.7)
Sex (n)	
Male	7 (58.3%)
Female	5 (41.7%)
Mean time since gastroenteropancreatic NET diagnosis (y)	4.8 (SD, 8.51)
Grade (n)	
Low	7 (58.3%)
Intermediate	5 (41.7%)
Gastroenteropancreatic NET hormonal status (n)	
Functioning	5 (41.7%)
Nonfunctioning	7 (58.3%)
sst analog (n)	
Yes (all long-acting somatostatin analogs)	6 (50%)
No	6 (50%)

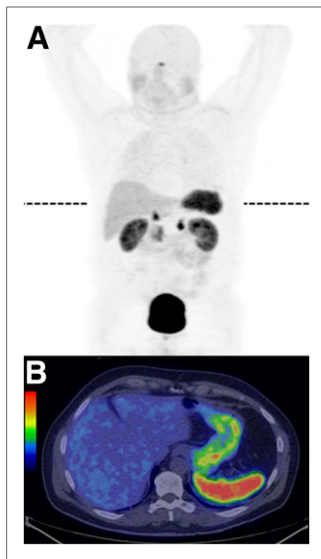


**FIGURE 1.** Biodistribution of 175 MBq of  $^{68}\text{Ga}$ -OPS202 (15  $\mu\text{g}$ ) 1 h after injection in patient 11 with NET of ileum. Currently, patient is in complete remission. (A) Whole-body PET scan. (B) Transaxial PET/CT slice at level of dashed line in A. There is low background activity in salivary glands, liver, and intestine.

To determine the optimal imaging time window, scans obtained at 0.5, 1, 2, and 4 h during visit 1 were evaluated according to the absolute numbers of detected lesions,  $\text{SUV}_{\text{max}}$  for tumors and for reference tissues, and mean image contrast values (tumor-to-background ratios:  $\text{SUV}_{\text{max}}$  of tumor to  $\text{SUV}_{\text{max}}$  of reference tissue). The evaluation was done by the central reader.

#### Radiation Dosimetry

For visit 1 (15- $\mu\text{g}$  peptide dose), organs with visible uptake were identified on PET images and delineated manually on PET/CT images

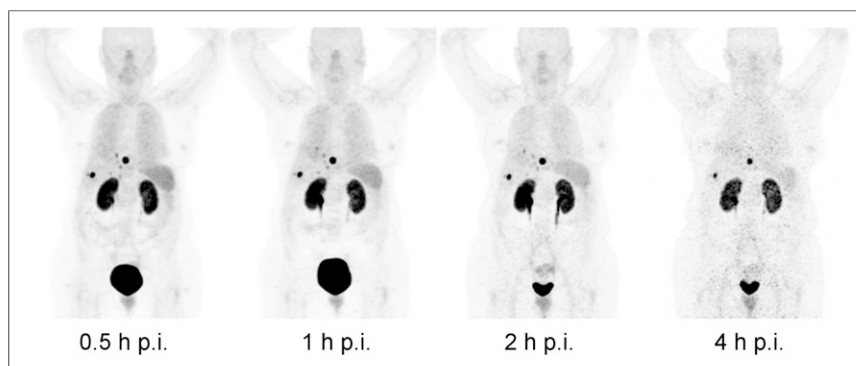


**FIGURE 2.** Biodistribution of 188 MBq of  $^{68}\text{Ga}$ -OPS202 (15  $\mu\text{g}$ ) at 0.5, 1, 2, and 4 h after injection in patient 2 with ileal NET. PET maximum-intensity projections with constant linear gray scale show multiple liver metastases and subdiaphragmatic peritoneal deposits. Tumor and renal uptake persists over time, whereas organs such as spleen, lungs, and liver, along with urinary excretion, are progressively washed out. Tumor contrast was highest at 1 h after injection, whereas 4-h images suffer from poor count statistics. Remarkably low accumulation of  $^{68}\text{Ga}$ -OPS202 is seen in  $\text{ss}2\text{t}$  receptor-positive organs such as pituitary, spleen, adrenals, and uncinate process of pancreas. p.i. = after injection.

region at 0.5, 1, 2, and 4 h after injection. At visit 2, a static scan was obtained from head to subinguinal region 1 h after injection.

#### Image Analysis

Two independent, qualified readers, one of whom was on-site (a board-certified nuclear medicine physician from University Hospital Basel) and the other central (a board-certified radiologist and nuclear medicine physician), masked to the patient and peptide dose, reviewed the scans. Each body region was assessed in the following order: liver, lymph nodes, bone, and other organs. Volumes of interest were used to measure  $\text{SUV}_{\text{max}}$  for each lesion and for reference tissue near the lesion. The biodistribution at 1 h after injection was compared between 15 and 50  $\mu\text{g}$  of  $^{68}\text{Ga}$ -OPS202 using  $\text{SUV}_{\text{max}}$  measured in the following normal organs: pituitary, parotid, thyroid, lung, mediastinum, liver, spleen, pancreas, stomach, jejunoleum, adrenals, and muscle.

using a prototype version of Mint Lesion (Mint Medical GmbH). Volumes of interest were drawn over the whole body and over the pituitary, parotids, thyroid, lungs, mediastinum, liver, pancreas, spleen, adrenals, kidneys, gastrointestinal tract, urinary bladder, and vertebral bodies L2–L4 to determine the relative activity in each organ at each time point. Patient-specific individual organ sizes taken from the CT scans were used to determine the uptake of the whole organ. No recovery correction was applied.

Time-activity curves (percentage injected activity within each volume of interest as a function of time) were derived, taking renal excretion of activity into account. With NUKFIT software (15), these curves were fitted by mono- or biexponential curves and integrated to yield the corresponding time-integrated activity coefficients (residence times). The absorbed radiation dose for each organ was calculated using the OLINDA dosimetry software (version 1.1) (16), according to the following parameters and assumptions:  $^{68}\text{Ga}$ ; adult male model; no bladder-voiding model; and equal distribution of residence times for the stomach, small intestine, upper large intestine, and lower large intestine. For bone marrow dosimetry, blood-based values for the red bone marrow residence times were calculated according to the method described by Herrmann et al. (17). In addition, an image-based red bone marrow residence time was calculated by integrating the L2–L4 time-activity curve, assuming that 6.7% of the total bone marrow is contained in L2–L4 (17).

Organ dose coefficients (mGy/MBq) were calculated, taking individual organ contributions into account as calculated by OLINDA. The effective dose per actual administered activity (mSv/MBq) was also calculated, applying the tissue weighting factors from publication 60 of the International Commission on Radiological Protection (18).

Blood samples were taken to determine time-activity curves before injection; at 2, 5, 10, 20, and 30 min after injection; and at 1, 2, and 4 h after injection. Urine was also collected—from 0 to 2 h after injection and from 2 to 4 h after injection—to determine the renal excretion of  $^{68}\text{Ga}$ . The total radioactivity concentration in whole blood and urine was determined using a  $\gamma$ -counter (Cobra II; Packard Instrument Co.).

#### Safety Assessments

The primary objective of the study was to evaluate the safety and tolerability of  $^{68}\text{Ga}$ -OPS202. These were assessed at visits 1, 2, and 3 by recording vital signs ( $\leq 4$  h after injection), physical examination findings, and clinical laboratory test results (hematology, biochemistry, urinalysis) at each visit and performing a 12-lead electrocardiogram (2.5 h after injection and at visit 3). Adverse events (AEs) were recorded and graded according to version 4.03 of the Common Terminology Criteria for Adverse Events.

#### Statistical Analysis

All variables were analyzed descriptively. The Wilcoxon signed-rank test, with a  $P$  value of less than 0.05 denoting statistical significance, was used to compare the 15- and 50- $\mu\text{g}$  doses (matched pairs).

## RESULTS

#### Patients

Twelve patients were screened and took part in the study. All completed the study and were included in the dosimetry, pharmacokinetic, and safety evaluations. Baseline demography and disease characteristics are summarized in Table 1 of this paper for the

**TABLE 2**

Mean Background Activity in Organs at 1 Hour After Injection of 15  $\mu\text{g}$  (Visit 1) and 50  $\mu\text{g}$  (Visit 2) of  $^{68}\text{Ga}$ -OPS202

Organ	SUV <sub>max</sub>		P
	Visit 1	Visit 2	
Liver	3.2 (0.8)	2.9 (0.7)	<0.05
Stomach	4.2 (2.3)	3.0 (1.2)	<0.05
Jejunioileum	3.5 (1.3)	2.9 (0.7)	<0.05
Pancreas	3.2 (2.0)	2.6 (1.4)	0.052
Parotids	3.7 (1.9)	3.4 (1.7)	0.06
Right adrenal	7.4 (3.7)	6.3 (2.3)	0.09
Left adrenal	8.3 (3.9)	7.1 (3.5)	0.08
Pituitary	5.8 (1.8)	5.7 (2.0)	0.23
Thyroid	2.3 (1.2)	2.3 (0.7)	0.93
Lung	1.7 (0.6)	1.6 (0.6)	0.29
Mediastinum	1.7 (0.5)	1.5 (0.3)	0.18
Spleen	11.7 (4.2)	10.1 (2.3)	0.14

Data in parentheses are SDs.

overall study population and in Table 1 of an accompanying paper (on phase II) for each patient (19).

#### Biodistribution and Pharmacokinetics

The mean residence time in the blood was  $2.4 \pm 1.1$  min/L. Figure 1 shows the whole-body biodistribution of  $^{68}\text{Ga}$ -OPS202 1 h after its injection in a patient with an ileal NET, who was in complete remission at the time of imaging. Figure 2 shows the whole-body biodistribution at 0.5, 1, 2, and 4 h in another patient with ileal NET.

Statistical analysis revealed subtle but significantly lower mean background activity (SUV<sub>max</sub>) at visit 2 (50- $\mu\text{g}$  dose) than at visit 1 (15- $\mu\text{g}$  dose) in the liver, stomach, and jejunioileum (Table 2).

#### Optimal Imaging Time Window

The overall number of malignant lesions at visit 1 was highest, with good reproducibility, in the 1- and 2-h scans and lowest in the 4-h scan: 152 (0.5 h), 162 (1 h), 164 (2 h), and 121 (4 h) (Fig. 2). Similarly, the total number of liver metastases was highest in the 1- and 2-h scans: 125 (0.5 h), 135 (1 h), 137 (2 h), and 96 (4 h). The total number of lymph node lesions remained almost constant: 19 in the first 3 scans and 18 in the 4-h scan.

For liver metastases, the time point at which most patients had the highest and most reproducible median image contrast (median tumor-to-background ratio with the normal liver as reference tissue) was 1 h (Fig. 2 and Supplemental Fig. 1; supplemental materials are available at <http://jnm.snmjournals.org>). This was also the case for lymph node metastases (normal lymph node as reference).

#### Radiation Dosimetry

Mean time-integrated activity coefficients and mean dose coefficients are shown in Tables 3 and 4, respectively. For calculation of the bone marrow contribution to the absorbed doses, the image-based residence times were used as a conservative estimate because they were generally higher than the corresponding blood-based

values. The organs with the largest time-integrated activity coefficients were the urinary bladder, liver, kidneys, and lung. The organs with the highest mean dose coefficients were the urinary bladder wall, kidneys, and spleen. The calculated mean effective dose was  $2.4\text{E}-02 \pm 0.2\text{E}-02$  mSv/MBq, which represents 3.6 mSv for a 150-MBq injection of  $^{68}\text{Ga}$ -OPS202.

#### Safety

Overall, 11 AEs were reported in 6 patients: grade 1 in 4 patients and grade 2 in 2 patients (Table 5). There were no grade 3 (severe), 4 (serious), or 5 (fatal) AEs.

The most frequently reported AEs were urinary tract infection and fatigue (Table 5). Three AEs in 2 patients were assessed as possibly related to treatment: eosinophilia, rash, and diarrhea. All were grade 1 in intensity, and none required drug treatment.

Overall, 8 patients had clinically significant abnormal laboratory results at least once during the study period. In most cases, these abnormalities were also documented either at screening or in the medical history. Furthermore, the number of patients with abnormal hematology, biochemistry, or urinalysis results did not increase from baseline over the course of the study, and no aggravating effect of  $^{68}\text{Ga}$ -OPS202 on already-abnormal renal or hepatic parameters was observed.  $^{68}\text{Ga}$ -OPS202 did not affect body weight, vital signs, the electrocardiogram results, or the physical examination results.

#### DISCUSSION

To our knowledge, this was the first clinical study to evaluate a  $^{68}\text{Ga}$ -labeled sst receptor antagonist for PET/CT imaging. The results showed that in patients with gastroenteropancreatic NETs,

**TABLE 3**

Mean Residence Time in Organs After Single Injection of  $^{68}\text{Ga}$ -OPS202

Organ	Residence time (min)
Whole body	80.22 (4.38)
Urinary bladder wall	5.16 (1.80)
Liver	4.32 (1.20)
Kidneys	3.42 (0.84)
Lung	2.64 (0.60)
Blood	2.40 (1.08)
Spleen	1.62 (1.02)
Red bone marrow*	1.32 (0.60)
Stomach	1.08 (0.18)
Lower large intestine	1.08 (0.18)
Upper large intestine	1.08 (0.18)
Small intestine	1.08 (0.18)
Heart	0.72 (0.24)
Pancreas	0.12 (0.06)
Vertebral bodies (L2–L4)	0.12 (0.06)
Adrenal glands	0.06 (0.000)
Gallbladder	0.06 (0.000)

\*Blood-based residence time calculation.  
Data in parentheses are SDs.

**TABLE 4**Mean Dose Coefficient in Organs After Single Injection of <sup>68</sup>Ga-OPS202

Organ	Dose coefficient (mGy/MBq)
Urinary bladder wall	1.01E-01 (4.28E-02)
Kidneys	8.43E-02 (3.13E-02)
Spleen	6.02E-02 (4.73E-02)
Lower large intestine wall	3.54E-02 (1.03E-02)
Adrenal glands	2.99E-02 (1.16E-02)
Upper large intestine wall	2.60E-02 (6.98E-03)
Stomach wall	2.30E-02 (7.53E-03)
Liver	2.18E-02 (8.66E-03)
Lung	2.12E-02 (7.01E-03)
Small intestine	1.89E-02 (4.50E-03)
Pancreas	1.55E-02 (5.09E-03)
Heart wall	1.47E-02 (3.83E-03)
Osteogenic cells	1.39E-02 (3.55E-03)
Gallbladder wall	1.22E-02 (3.10E-03)
Uterus	1.19E-02 (1.72E-03)
Red marrow	1.13E-02 (3.08E-03)
Ovaries	1.10E-02 (1.68E-03)
Testes	8.52E-03 (1.70E-03)
Muscle	8.50E-03 (1.68E-03)
Thymus	8.41E-03 (1.73E-03)
Thyroid	8.04E-03 (1.73E-03)
Breasts	7.45E-03 (1.70E-03)
Brain	7.32E-03 (1.72E-03)
Skin	7.13E-03 (1.69E-03)

Data in parentheses are SDs.

the organs with the highest dose coefficients were the bladder wall, kidneys, and spleen. The results obtained for the bladder wall and kidneys were consistent with this class of compounds and with the renal elimination of <sup>68</sup>Ga-OPS202.

Data from dosimetry studies with <sup>68</sup>Ga-labeled sst receptor agonists (<sup>68</sup>Ga-DOTATOC, <sup>68</sup>Ga-DOTATATE, and <sup>68</sup>Ga-DOTANOC) and the results from the current study showed comparable calculated mean effective doses: 2.4E-02 ± 0.2E-02 mSv/MBq for <sup>68</sup>Ga-OPS202, 2.6E-02 ± 0.3E-02 mSv/MBq and 2.1E-02 ± 0.3E-02 mSv/MBq for <sup>68</sup>Ga-DOTATATE (20,21), 2.1E-02 ± 0.3E-02 mSv/MBq for <sup>68</sup>Ga-DOTATOC (21), and 2.5E-02 ± 0.5E-02 mSv/MBq for <sup>68</sup>Ga-DOTANOC (22). However, there were differences in the biodistribution among these tracers resulting in different organ doses. The most pronounced differences were for the liver, lung, and spleen. The mean liver dose was 2.2E-02 ± 0.9E-02 mGy/MBq for <sup>68</sup>Ga-OPS202, 4.5E-02 ± 1.5E-02 and 5.0E-02 ± 1.5E-02 mGy/MBq for <sup>68</sup>Ga-DOTATATE (20,21), 4.1E-02 ± 1.4E-02 mGy/MBq for <sup>68</sup>Ga-DOTATOC (21), and 3.4E-02 ± 1.0E-02 mGy/MBq for <sup>68</sup>Ga-DOTANOC (22). The low liver uptake and dose of <sup>68</sup>Ga-OPS202 are likely to be clinically relevant because, compared with <sup>68</sup>Ga-DOTATOC, <sup>68</sup>Ga-OPS202 exhibits substantially higher tumor-to-background ratios and sensitivity for detecting liver metastases (as described in the accompanying paper (19)). The mean lung dose

was 2.1E-02 ± 0.7E-02 mGy/MBq for <sup>68</sup>Ga-OPS202 and between 0.6E-03 and 1.2E-02 mGy/MBq for <sup>68</sup>Ga-labeled sst receptor agonists.

Slight differences in biodistribution were observed between the 2 doses of <sup>68</sup>Ga-OPS202 (15 and 50 µg) 1 h after injection. With the higher peptide amount, the liver, stomach, intestine, and pancreas showed either a trend toward lower background uptake or significantly lower background uptake. The reason for this finding in the liver, reputed to be sst<sub>2</sub> receptor-negative, is unknown, and there are notable exceptions among sst<sub>2</sub> receptor-expressing organs (e.g., the pituitary and the adrenals, possibly because of their small size and the high partial-volume effects affecting the accuracy of the uptake measure). In any case, this lower background activity is an important feature, as it may improve tumor detection in organs that are potential sites of primary or metastatic disease. However, this finding did not translate into significantly different tumor-to-background ratios or significantly different numbers of detected metastases (when the on-site reader only was considered) between the 2 peptide doses, probably because of the small difference in the amount of peptide and the limited sample size. Nevertheless, this finding suggests that saturation of physiologically expressed sst<sub>2</sub> receptors in organs occurs at an early stage of dose escalation and is consistent with the results of our preclinical evaluation using larger peptide amounts (23).

The current study also evaluated the optimal imaging time window for <sup>68</sup>Ga-OPS202. Based on image contrast data, number of detected lesions, and reproducibility, the optimal window is between 1 and 2 h. PET/CT scans for other <sup>68</sup>Ga-labeled sst ligands are also acquired at approximately 1 h (24).

The administration of <sup>68</sup>Ga-OPS202 was well tolerated. Most AEs were grade 1, and there were no grade 3, 4, or 5 AEs. Furthermore, there were no signals of concern from any of the laboratory blood test or urinalysis results. When abnormal laboratory findings were reported, most were related to underlying disease (e.g., chronic kidney disease or diabetes mellitus) or to urinary tract infection. Three AEs were assessed as being possibly related to treatment: grade 1 eosinophilia in one patient, and rash and

**TABLE 5**Summary of AEs After Single Dose of <sup>68</sup>Ga-OPS202

Patient no.	AE	Intensity*	Relationship
1	Urinary tract infection	Grade 2	Unlikely
3	Abdominal pain	Grade 1	Not related
	Urinary tract infection	Grade 1	Not related
	Abnormal liver function test	Grade 1	Unlikely
5	Eosinophilia	Grade 1	Possible
	Fatigue	Grade 1	Unlikely
7	Fatigue	Grade 2	Unlikely
8	Nasopharyngitis	Grade 1	Not related
11	Rash	Grade 1	Possible
	Diarrhea	Grade 1	Possible
	Headache	Grade 1	Unlikely

\*According to version 4.03 of the Common Terminology Criteria for Adverse Events.

diarrhea (both grade 1) in another. Mild hypereosinophilia is a nonspecific finding that may accompany a number of conditions (e.g., infections, asthma and allergies, vasculitis, and nonhematologic malignancies) but also can occur as a drug reaction. Other  $^{68}\text{Ga}$ -labeled sst analogs are also well tolerated. No clinical adverse reactions were reported for  $^{68}\text{Ga}$ -DOTATOC (22) or for  $^{68}\text{Ga}$ -DOTATATE, and there were no changes in physiologic responses, blood counts, electrolytes, liver function test results, or renal function (20).

One of the limitations of the study was the small patient number, which is, however, typical for this stage of early drug development. The number of patients evaluated in dosimetry studies on the  $^{68}\text{Ga}$ -labeled sst receptor agonists was also small ( $n = 6\text{--}10$ ) (20–22). Other limitations related to the study design. First, the crossover design was not 2-way; that is, none of the patients received the higher peptide dose first. Second, extended follow-up was not conducted to evaluate the longer-term safety profile of  $^{68}\text{Ga}$ -OPS202. However, long-term safety is not expected to be an issue given the short half-life of the radionuclide, the low radiation burden, and the low amount of peptide, which is likely to be too low to exert pharmacologic activity. The main strength of the study was the use of PET/CT-based 3-dimensional dosimetry, which allows higher spatial resolution and more precise delineation of organ-bound activity than 2-dimensional dosimetry.

## CONCLUSION

This phase I study showed that  $^{68}\text{Ga}$ -OPS202 is rapidly cleared from the blood, resulting in low background activity, especially in the liver and gastrointestinal tract. Accordingly, administration of  $^{68}\text{Ga}$ -OPS202 delivers an acceptable radiation dose to organs. The effective dose is comparable to  $^{68}\text{Ga}$ -labeled sst receptor agonists that are already established in the clinic, and there were no safety signals of concern. Further evaluation of  $^{68}\text{Ga}$ -OPS202 for PET/CT imaging of NETs and other sst<sub>2</sub> receptor-expressing tumors is therefore warranted.

## DISCLOSURE

Jean E.F. Rivier, Jean Claude Reubi, and Helmut R. Maecke, who are coinventors of sst receptor-based antagonistic radiopeptides, assigned all their patent rights to their respective academic institution. Hakim Bouterfa is a founder of OctreoPharm Sciences GmbH and a former employee of Ipsen; he now acts as a consultant for Ipsen. Jens Kaufmann is an employee of Ipsen. Medical writing support was funded by Ipsen. This study was sponsored by Ipsen. Jean E.F. Rivier receives funding through the “Dr. Frederik Paulsen Chair in Neurosciences Professor” award. No other potential conflict of interest relevant to this article was reported.

## ACKNOWLEDGMENTS

We thank all the patients who participated in the trial, the OctreoPharm/Ipsen team, the personnel of the Division of Radiopharmaceutical Chemistry and Nuclear Medicine at University Hospital Basel, and John Uiters and Nils Schreiter from Medwave Medical Imaging. We thank Judit Erchegeyi, Charleen Miller, and Josef Gulyas for their early contribution to the synthesis and characterization of the peptide reagents. We also thank Nicky French (Watermeadow Medical) for medical writing support.

## REFERENCES

1. Cives M, Strosberg J. An update on gastroenteropancreatic neuroendocrine tumors. *Oncology (Williston Park)*. 2014;28:749–756, 758.
2. Modlin IM, Moss SF, Chung DC, Jensen RT, Snyderwine E. Priorities for improving the management of gastroenteropancreatic neuroendocrine tumors. *J Natl Cancer Inst*. 2008;100:1282–1289.
3. Pavel M, O'Toole D, Costa F, et al. ENETS consensus guidelines update for the management of distant metastatic disease of intestinal, pancreatic, bronchial neuroendocrine neoplasms (NEN) and NEN of unknown primary site. *Neuroendocrinology*. 2016;103:172–185.
4. Reubi JC, Waser B. Concomitant expression of several peptide receptors in neuroendocrine tumours: molecular basis for in vivo multireceptor tumour targeting. *Eur J Nucl Med Mol Imaging*. 2003;30:781–793.
5. Werner RA, Bluemel C, Allen-Auerbach MS, Higuchi T, Herrmann K.  $^{68}\text{Ga}$ -gallium- and  $^{90}\text{Y}$ -lutetium- $^{177}\text{Lu}$ -DOTA: “theranostic twins” for diagnosis and treatment of NETs. *Ann Nucl Med*. 2015;29:1–7.
6. Gabriel M, Decristoforo C, Kendler D, et al.  $^{68}\text{Ga}$ -DOTA-Tyr3-octreotide PET in neuroendocrine tumors: comparison with somatostatin receptor scintigraphy and CT. *J Nucl Med*. 2007;48:508–518.
7. Reubi JC, Schar JC, Waser B, et al. Affinity profiles for human somatostatin receptor subtypes SST1–SST5 of somatostatin radiotracers selected for scintigraphic and radiotherapeutic use. *Eur J Nucl Med*. 2000;27:273–282.
8. Poeppel TD, Binse I, Petersenn S, et al.  $^{68}\text{Ga}$ -DOTATOC versus  $^{68}\text{Ga}$ -DOTA-TATE PET/CT in functional imaging of neuroendocrine tumors. *J Nucl Med*. 2011; 52:1864–1870.
9. Ruf J, Schiefer J, Furth C, et al.  $^{68}\text{Ga}$ -DOTATOC PET/CT of neuroendocrine tumors: spotlight on the CT phases of a triple-phase protocol. *J Nucl Med*. 2011; 52:697–704.
10. Ginj M, Zhang H, Waser B, et al. Radiolabeled somatostatin receptor antagonists are preferable to agonists for in vivo peptide receptor targeting of tumors. *Proc Natl Acad Sci USA*. 2006;103:16436–16441.
11. Wild D, Fani M, Behe M, et al. First clinical evidence that imaging with somatostatin receptor antagonists is feasible. *J Nucl Med*. 2011;52:1412–1417.
12. Cescaio R, Erchegeyi J, Waser B, et al. Design and in vitro characterization of highly sst2-selective somatostatin antagonists suitable for radiotargeting. *J Med Chem*. 2008;51:4030–4037.
13. Fani M, Braun F, Waser B, et al. Unexpected sensitivity of sst2 antagonists to N-terminal radiometal modifications. *J Nucl Med*. 2012;53:1481–1489.
14. Mueller D, Klette I, Baum RP, Gottschaldt M, Schultz MK, Breeman WA. Simplified NaCl based  $^{68}\text{Ga}$  concentration and labeling procedure for rapid synthesis of  $^{68}\text{Ga}$  radiopharmaceuticals in high radiochemical purity. *Bioconjug Chem*. 2012;23:1712–1717.
15. Kletting P, Schimmel S, Kestler HA, et al. Molecular radiotherapy: the NUKFIT software for calculating the time-integrated activity coefficient. *Med Phys*. 2013; 40:102504.
16. Stabin MG, Sparks RB, Crowe E. OLINDA/EXM: the second-generation personal computer software for internal dose assessment in nuclear medicine. *J Nucl Med*. 2005;46:1023–1027.
17. Herrmann K, Lapa C, Wester HJ, et al. Biodistribution and radiation dosimetry for the chemokine receptor CXCR4-targeting probe  $^{68}\text{Ga}$ -pentixafor. *J Nucl Med*. 2015;56:410–416.
18. 1990 recommendations of the International Commission on Radiological Protection: ICRP publication 60. *Ann ICRP*. 1991;21.
19. Nicolas GP, Schreiter N, Kaul F, et al. Sensitivity comparison of  $^{68}\text{Ga}$ -OPS202 and  $^{68}\text{Ga}$ -DOTATOC PET/CT in patients with gastroenteropancreatic neuroendocrine tumors: a prospective phase II imaging study. *J Nucl Med*. 2018;59:915–921.
20. Walker RC, Smith GT, Liu E, Moore B, Clanton J, Stabin M. Measured human dosimetry of  $^{68}\text{Ga}$ -DOTATATE. *J Nucl Med*. 2013;54:855–860.
21. Sandström M, Veliky I, Garske-Roman U, et al. Comparative biodistribution and radiation dosimetry of  $^{68}\text{Ga}$ -DOTATOC and  $^{68}\text{Ga}$ -DOTATATE in patients with neuroendocrine tumors. *J Nucl Med*. 2013;54:1755–1759.
22. Pettinato C, Sarnelli A, Di Donna M, et al.  $^{68}\text{Ga}$ -DOTANOC: biodistribution and dosimetry in patients affected by neuroendocrine tumors. *Eur J Nucl Med Mol Imaging*. 2008;35:72–79.
23. Nicolas GP, Mansi R, McDougall L, et al. Biodistribution, pharmacokinetics, and dosimetry of  $^{177}\text{Lu}$ -,  $^{90}\text{Y}$ - and  $^{111}\text{In}$ -labeled somatostatin receptor antagonist OPS201 in comparison to the agonist  $^{177}\text{Lu}$ -DOTATATE: the mass effect. *J Nucl Med*. 2017;58:1435–1441.
24. Virgolini I, Ambrosini V, Bomanji JB, et al. Procedure guidelines for PET/CT tumour imaging with  $^{68}\text{Ga}$ -DOTA-conjugated peptides:  $^{68}\text{Ga}$ -DOTA-TOC,  $^{68}\text{Ga}$ -DOTA-NOC,  $^{68}\text{Ga}$ -DOTA-TATE. *Eur J Nucl Med Mol Imaging*. 2010;37:2004–2010.